Ultrasound in Med. & Biol., Vol. 46, No. 8, pp. 2007–2016, 2020

0301-5629/$ - see front matter

https://doi.org/10.1016/j.ultrasmedbio.2020.04.023

● *Original Contribution*

EFFECT OF STIFFNESS OF LARGE EXTRAVASCULAR HEMATOMAS ON THEIR SUSCEPTIBILITY TO BOILING HISTOTRIPSY LIQUEFACTION *IN VITRO*

TATIANA D. KHOKHLOVA,* JOHN C. KUCEWICZ,† EKATERINA M. PONOMARCHUK,‡ CHRISTOPHER HUNTER,† MATTHEW BRUCE,† VERA A. KHOKHLOVA,†,‡ THOMAS J. MATULA,† and WAYNE MONSKY§

* Department of Medicine, University of Washington, Seattle, Washington, USA; † Center for Industrial and Medical Ultrasound, Applied Physics Lab, University of Washington, Seattle, Washington, USA; ‡ Physics Faculty, Lomonosov Moscow State University, Moscow, Russia; and § Department of Radiology, University of Washington, Seattle, Washington, USA

(*Received* 14 *January* 2020; *revised* 31 *March* 2020; *in final from* 20 *April* 2020)

Abstract—Large intra-abdominal, retroperitoneal and intramuscular hematomas are common consequences of sharp and blunt trauma and post-surgical bleeds, and often threaten organ failure, compartment syndrome or spontaneous infection. Current therapy options include surgical evacuation and placement of indwelling drains that are not effective because of the viscosity of the organized hematoma. We have previously reported the feasibility of using boiling histotripsy (BH)—a pulsed high-intensity focused ultrasound method—for liquefaction of large volumes of freshly coagulated blood and subsequent fine-needle aspiration. The goal of this work was to evaluate the changes in stiffness of large coagulated blood volumes with aging and retraction *in vitro*, and to correlate these changes with the size of the BH void and, therefore, the susceptibility of the material to BH liquefaction. Large-volume (55–200 mL) whole-blood clots were fabricated in plastic molds from human and bovine blood, either by natural clotting or by recalcification of anticoagulated blood, with or without addition of thrombin. Retraction of the clots was achieved by incubation for 3 h, 3 d or 8 d. The shear modulus of the samples was measured with a custom-built indentometer and shear wave elasticity (SWE) imaging. Sizes of single liquefied lesions produced with a 1.5-MHz high-intensity focused ultrasound transducer within a 30-s standard BH exposure served as the metric for susceptibility of clot material to this treatment. Neither the shear moduli of naturally clotted human samples (0.52 ± 0.08 kPa), nor their degree of retraction (ratio of expelled fluid to original volume 50%–58%) depended on the length of incubation within 0–8 d, and were significantly lower than those of bovine samples (2.85 ± 0.17 kPa, retraction 5%–38%). In clots made from anticoagulated bovine blood, the variation of calcium chloride concentration within 5–40 mmol/L did not change the stiffness, whereas lower concentrations and the addition of thrombin resulted in significantly softer clots, similar to naturally clotted human samples. Within the achievable shear modulus range (0.4–1.6 kPa), the width of the BH-liquefied lesion was more affected by the changes in stiffness than the length of the lesion. In all cases, however, the lesions were larger compared with any soft tissue liquefied with the same BH parameters, indicating higher susceptibility of hematomas to BH damage. These results suggest that clotted bovine blood with added thrombin is an acceptable *in vitro* model of both acute and chronic human hematomas for assessing the efficiency of BH liquefaction strategies. (E-mail: tdk7@uw.edu)

Key Words: **Sonothrombolysis, High-intensity focused ultrasound, Boiling histotripsy, Hematoma, Clot, Elastography, Elastic modulus, Stiffness.**

INTRODUCTION

Clinical management of large (hundreds of milliliters to liters in volume) intra-abdominal, retroperitoneal and intramuscular hematomas in trauma and post-surgical care depends on the size and location of the hematoma and includes conservative treatment, drainage through percutaneously placed indwelling drains and surgical evacuation. Hematomas do liquefy and resorb on their own with a conservative approach, but this process typically takes multiple weeks and is not a viable option for symptomatic painful hematomas or those threatening compartment syndrome or organ failure. Drainage catheter placement is minimally effective because of the gelatinous nature of the acute and subacute hematoma, and may be only beneficial for older, more liquefied, hematomas. This approach can be associated with significant morbidity, and frequently leads to infection of a

Address correspondence to: Tatiana D. Khokhlova, Box 359773, 325 Ninth Avenue, Seattle, WA 98104, USA. E-mail: tdk7@uw.edu

sterile hematoma (Weiss et al. 2015). Surgical evacuation can be an extensive and morbid procedure, which represents the last resort, but also is the only truly effective approach to evacuating the hematoma.

The feasibility of using a non-invasive high-intensity focused ultrasound (HIFU)-based technique—histotripsy—for rapid liquefaction of large hematomas and subsequent aspiration through a fine needle both *in vitro* and *in vivo* was recently reported (Khokhlova et al. 2016; Looi et al. 2016; Gerhardson et al. 2017, 2020). One histotripsy technique termed *boiling histotripsy* (BH) uses millisecond-long burst pulses of non-linear HIFU to induce vapor and cavitation bubble activity at the focus and, thus, liquefy tissue or other gel-like materials, including hematomas (Khokhlova et al. 2016). As reported in the *in vitro* experiments with large volumes of freshly clotted bovine blood, ultrasound-guided BH exposures provided liquefaction rates approaching clinical requirements. However, the liquefaction rate for any histotripsy technique, including BH, is known to be inversely dependent on the material stiffness, that is, elastic modulus (Vlaisavljevich et al. 2014; Wang et al. 2018). For intravascular clots *in vivo,* it was found that their elastic modulus increased with time because of retraction (or syneresis) of the fibrin network, infiltration by leukocytes and, ultimately, replacement of fibrin by collagen (Xie et al. 2005). The elastic properties and microscopic structure of *in vitro* models of intravascular clots, both fresh and retracted, have been reported in multiple studies (Chueh et al. 2011; Sutton et al. 2013; Mercado-Shekhar et al. 2018). In particular, measurements of Young's modulus of *in vitro* clot models with shear wave elastography (SWE) were reported during and after intravascular clot retraction (Zhang et al. 2016; Mercado-Shekhar et al. 2018). The feasibility and high efficiency of histotripsy liquefaction of intravascular clots have been reported both *in vivo* and *in vitro*, with and without addition of recombinant tissue plasminogen activator, and the lysis rate was substantially lower for retracted versus un-retracted clots (Zhang et al. 2016, 2017; Bollen et al. 2019).

The natural progression of larger-volume, extravascular hematomas is less well described compared with that of intravascular clots. Acute hematomas (1−2 d old) are known to be uniformly gelatinous, and SWE measurements of Young's modulus during large clot formation *in vitro* were previously reported (Bernal et al. 2012). Subacute and chronic hematomas (weeks to months) separate into an organized, gelatinous fraction and serous, fluid fraction, the latter drainable through the indwelling catheter. For further development and clinical translation of ultrasound-guided BH for hematoma liquefaction, it is important to characterize the susceptibility of not only acute, but also organized chronic hematoma to this type of mechanical damage. Because the organized fraction of chronic hematoma is not as accessible to infiltrating fibroblasts as the narrow intravascular clot, the fibrin matrix is not replaced by collagen as readily, and the clot eventually resolves completely because of the activity of neutrophils and macrophages trapped within the clotted volume from the beginning and/or gradually infiltrating the volume over time (Rao et al. 2016a).

In the study described here, we aimed to mimic the process of human hematoma aging *in vitro* by incubating freshly clotted human blood for several days to allow for consistent retraction and to directly measure the associated changes in its stiffness over the incubation time. These stiffness changes would be compared with those in the more accessible clotted bovine blood samples undergoing the same incubation process, to test the relevance of using them as phantoms for BH exposures, as done in our previous studies (Khokhlova et al. 2016). The next goal was to match the shear moduli of the naturally clotted human hematomas and the bovine blood phantoms by using anticoagulated bovine blood and adding varying concentrations of thrombin and calcium chloride ($CaCl_2$), which are known to change the structure of the fibrin network at the microscopic level (Nogueira 2012; Sutton et al. 2013; Ryan et al. 1999). The ultimate goal was to correlate the size and shape of liquefied lesions produced in the *in vitro* bovine blood phantoms using a standard BH exposure with their stiffness, within the stiffness range measured for *in vitro* human hematoma samples.

METHODS

In vitro *hematoma models*

Bovine hematoma phantoms were made at the University of Washington using bovine blood obtained from a local abattoir. The blood was either poured into plastic containers and allowed to clot naturally at room temperature for 3 h or anticoagulated with citrate−phosphate−dextrose (CPD, No. C7165; Millipore-Sigma, St. Louis, MO, USA) at a 9:1 volume ratio. Before the experiments, anticoagulated blood was poured into plastic molds and degassed at room temperature for at least 1 h. Coagulation was achieved by adding 1 mol/L of a solution of $CaCl_2$ (No. C3306, Millipore-Sigma) and bovine thrombin (No. T4648, Millipore-Sigma) at different concentrations and incubating the samples at 36°C for 3 h. The phantoms were kept refrigerated and examined within a week.

Plastic container molds of two different sizes were used: larger, rectangular acrylic containers 200 mL in volume ($6 \times 6 \times 5.5$ cm) for the samples that were treated with BH, or cylindrical polypropylene containers 55 mL in volume (4 cm in diameter, 4 cm high) for the samples that were used only for measurement of the elastic modulus (Fig. 1). For shear wave elastography (SWE) imaging, a larger volume sample was prepared: 700 mL of anticoagulated blood was poured into a large latex balloon, $CaCl_2$ solution was added and gently mixed and

Fig. 1. (a) Schematic of the custom-built indentometer used to measure the shear modulus of large-volume human and bovine blood clot samples. The indenter tip was a hard sphere with an $R = 4.75$ mm radius. The sample surface displacement, d, was controlled by a linear positioning stage, and the resulting force was measured by laboratory scale. The shear modulus was calculated from the linear fit of the displacement–force relationship. (b) Bovine and (c) human clotted blood sample before (left) and after (right) retraction/syneresis, that is, shrinkage accompanied by expulsion of translucent liquid. Bars = 2 cm.

the balloon was sealed without trapping air. The sample was incubated in the refrigerator for 3 d to ensure retraction before it was imaged using the Aixplorer ultrasound imaging platform (Supersonic Imagine, Aix-en-Provence, France).

The *in vitro* human hematoma samples were prepared and examined at Lomonosov Moscow State University for shear modulus measurement only. In the first set of measurements, fresh blood without anticoagulant was collected from healthy volunteers through sterile venipuncture according to the guidelines of the Dmitry Rogachev National Research Center. The blood was poured into cylindrical polypropylene containers (55-mL volume) and allowed to clot naturally at room temperature for 3 h. In the second set of measurements, random donor blood units stabilized with standard citrate anticoagulant, CPD, were obtained from the Blood Bank Department of the Center and used without authentication. The anticoagulated blood was poured into the same molds, de-gassed in a desiccant chamber for 1 h, recalcified with $CaCl_2$ solution to a final concentration of 25 mmol/L and incubated for 3 h at room temperature. All samples were then kept refrigerated and examined within a week.

Measurement of clot shear and elastic moduli

In present work, the Poisson ratio of the clot material was considered to be close to 0.5, as commonly assumed for soft tissues (Szabo 2004), and therefore, the elastic modulus (or Young's modulus) was assumed to be three times the shear modulus. Shear moduli of the clot samples were measured using a custom-built indentometer (Fig. 1a), in which a rigid spherical indenter was used to displace the sample surface, while measuring the resulting force on the sample. The shear modulus was calculated from the force–displacement relationship for a spherical indenter, which can be expressed analytically under the following conditions: the medium is isotropic, linearly elastic and incompressible, and the contact radius and the displacement are small compared with the sample size (Choi and Shield 1981):

$$F^{\frac{2}{3}} = \left(\frac{16\mu}{3}\right)^{\frac{2}{3}} R^{\frac{1}{3}} d \qquad (1)$$

Here, F is the force, d is the sample surface displacement, R is the indenter radius and μ is the shear modulus. In the present setup, an 8-mm-diameter steel ball attached to a linear positioning system was used as the indenter, and the maximum displacement did not exceed 2 mm, achieved in 0.1-mm steps. The force was measured with an electronic scale (Acculab ALC-320-3; Sartorius Mechatronics Corp., Bohemia, NY, USA). Shear modulus for each sample was calculated using eqn (1) from the linear fit of the obtained force–displacement relationship. This measurement approach was successfully used previously to characterize the elastic moduli of tissue-mimicking phantoms (Dunmire et al. 2013), and the uncertainty was reported to be 10%.

For shear modulus measurement, the hematoma samples (Fig. 1b, 1c) were gently removed from the mold. To quantify the degree of retraction or syneresis, the translucent liquid fraction was first carefully drained into the graduated cylinder and its volume was recorded. The remaining organized (*i.e.,* gel-like, solid) fraction was placed on the scale, and shear modulus measurements were then taken in at least three points on different sides of the sample and averaged. The goodness-of-fit coefficient R^2 for the force–displacement relationship according to eqn (1) was better than 0.99 for all samples.

As mentioned above, hematoma stiffness obtained from indentometer measurement has a value averaged over the sample volume, provided that the sample is fairly uniform. To verify this assumption and validate the stiffness measurements, SWE imaging of a large-volume sample was performed using the Aixplorer imaging system with a curvilinear XC6-1 probe (Supersonic Imagine). Multiple (n = 12) images were recorded throughout the volume of the sample, and values of the elastic (Young's) modulus were taken within small regions of interest (ROIs) in each image. Shear modulus was then calculated by dividing the obtained elastic modulus values by a factor of 3 and averaged across all ROIs. Immediately after SWE imaging, the organized fraction of the sample was removed from the balloon that contained it and separated into five segments, and the shear modulus of each segment was measured with the indentometer as previously described.

Boiling histotripsy setup and exposures

Exposures of the hematoma samples to BH were performed in a tank filled with de-gassed, de-ionized water, using a 1.5-MHz HIFU transducer with 75-mm aperture and radius of curvature, consisting of 12 sector elements (Khokhlova et al. 2016). The transducer had a central opening that incorporated an ultrasound imaging probe for treatment guidance and targeting (P7-4 probe, Sonix RP, Ultrasonix, Richmond, BC, Canada) and was driven by custom-built high-power electronics (Maxwell et al. 2017).

For the BH treatment, the hematoma sample was inserted in a holder attached to a computer-controlled 3-D positioning system and placed in a tank with de-ionized water, as illustrated schematically in Figure 2a. A thin plastic bag filled with de-gassed saline was placed around the sample to avoid rupture of red blood cells in the phantom and contamination of the de-ionized water in the tank. The HIFU focus pre-registered with the imaging system was positioned at a depth of 1.5−2 cm under the surface of the hematoma sample, and BH exposures were delivered to a grid of locations in the phantom. After the exposures, the sample was imaged with a higher-resolution ultrasound probe (L14-5, Sonix RP, Ultrasonix), then bisected along the HIFU propagation axis and photographed.

All locations in all samples in this work received the same BH exposure, with the following parameters: pulse duration of 10 ms, pulse repetition frequency of 1 Hz, exposure duration of 30 s corresponding to 30 delivered BH pulses, peak acoustic power of 400 W. The corresponding focal waveform, as measured with the fiber-optic probe hydrophone in water and de-rated into the clot sample, is illustrated in Figure 2b. Non-linear de-rating was performed based on measured focal waveforms in water at increasing transducer output levels and then according to a previously developed de-rating method (Bessonova O et al., 2010; Khokhlova et al. 2016). The method accounts for differences in absorption and non-linearity of water and coagulated blood. The shock front of 83-MPa amplitude was sufficient to induce boiling in the clot material within 2.3 ms, according to weak shock theory-based estimation, similarly to our prior studies (Khokhlova et al. 2016).

RESULTS

Shear moduli of human and bovine clot samples

The results of shear modulus measurements with the indentometer are illustrated in Figure 3. As seen, shear moduli of neither freshly clotted bovine, nor human blood, nor recalcified anticoagulated human blood changed significantly over the incubation period of 1 wk, and were confined within a fairly narrow range of 0.75−1.1 kPa for bovine and 0.41−0.62 kPa for human samples, regardless of whether they were made of freshly coagulated or anticoagulated/recalcified blood (Fig. 3a). Clots made with bovine blood had a significantly higher shear modulus (*i.e.,* were stiffer) than human clots at all time points, which is in agreement with other studies examining interspecies differences in blood clotting parameters (Mercado-Shekhar et al. 2018; Mizuno et al. 2018). On average, the shear modulus values for human samples were lower than those reported by Mercado-Shekhar et al. (2018) for fully retracted intravascular *in vitro* human clot models (1.07 ± 0.6 kPa). The shear modulus values for bovine samples were also lower than those reported by (Zhang et al. 2016) for fully retracted intravascular *in vitro* clot models made of bovine blood (3.6 ± 0.5 kPa).

The degree of retraction, that is, the volume ratio of the serous fraction to the original blood volume, ranged from 5%−38% for bovine blood and from 50%−58% for human blood, and did not significantly depend on the length of incubation (*i.e.,* most retraction occurred within the first 3 h after coagulation, before the first measurement of the shear modulus). Measured shear modulus of the organized fraction of the samples did not correlate with the degree of retraction in any of the groups. This observation differs from that of the retracted intravascular clot *in vitro* model reported by Zhang et al. (2016), where Young's modulus for un-retracted clots was measured to be almost six times smaller than that for the retracted clots. We hypothesize that this difference can be explained by the dependence of clot retraction (or syneresis) dynamics on the clot volume and shape- or surface-to-volume ratio: small-volume (typically <10 mL), long and narrow intravascular clots versus larger-volume (>50 mL) clots with approximately equal dimensions used in this study to mimic large hematomas. The kinetics of syneresis—spontaneous contraction of gels (of

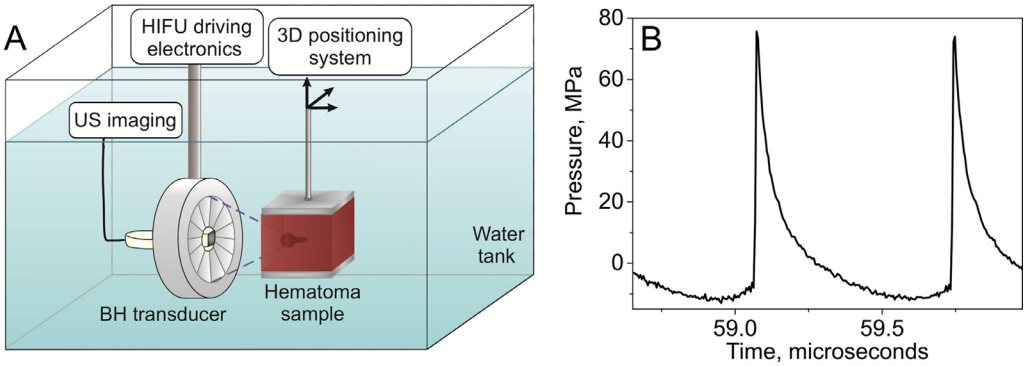

Fig. 2. (a) Diagram and photo of the boiling histotripsy (BH) setup used to liquefy hematoma samples. The 1.5-MHz high-intensity focused ultrasound transducer consisting of 12 sector elements was integrated with an ultrasound1 imaging probe in the central opening of the transducer for BH guidance during exposures. (b) Focal ultrasound waveform corresponding to the output used for BH exposures, measured in water with a fiber-optic probe hydrophone and de-rated into bovine clot. US = ultrasound.

which a blood clot is one example) accompanied by expulsion of liquid from the pores—is known to be dependent on the size and shape of the gel, because small pores resist the flow of fluid out of the gel more noticeably over larger gel dimensions (Pickering and Hewitt 1923; Scherer 1989).

The shear modulus of anticoagulated bovine blood samples was dependent on the concentration of $CaCl_2$ that was added for clotting (Fig. 3b). A low concentration of 1.5 mmol/L led to formation of either a very soft clot or completely liquid sample, resulting in a significantly lower mean shear modulus compared with the clots obtained at calcium chloride concentrations of 5−40 mmol/L. Interestingly, further increase in $CaCl_2$ concentration beyond 50 mmol/L led to a significant decrease in the shear modulus and/or inconsistent clotting, similar to that obtained with low $CaCl_2$ concentration. If $CaCl_2$ concentration was intermediate (25 mmol/L), adding varying concentrations of thrombin did not significantly affect the clot's shear modulus (Fig. 3c). At low $CaCl_2$ concentration, however, the addition of thrombin led to the increase in shear modulus up to the values obtained from freshly coagulated blood.

As seen from Figure 3, the shear moduli of naturally clotted human and bovine blood differ for all incubation durations, but both can be recapitulated by using anticoagulated bovine blood recalcified with $CaCl_2$ and adding thrombin. Specifically, the shear modulus range of retracted bovine hematomas is best recapitulated with the protocol in which only calcium chloride is added to anticoagulated bovine blood, at the concentration of 25 mmol/L. This concentration is also close to that used by other groups that have explored the use of ultrasound for sonothrombolysis (Sutton et al. 2013; Zhang et al. 2015, 2016). The shear modulus range of retracted human clots is best matched by adding a low concentration of $CaCl_2$ (1.5 mmol/L) and thrombin within the 1−5 NIHU/mL range.

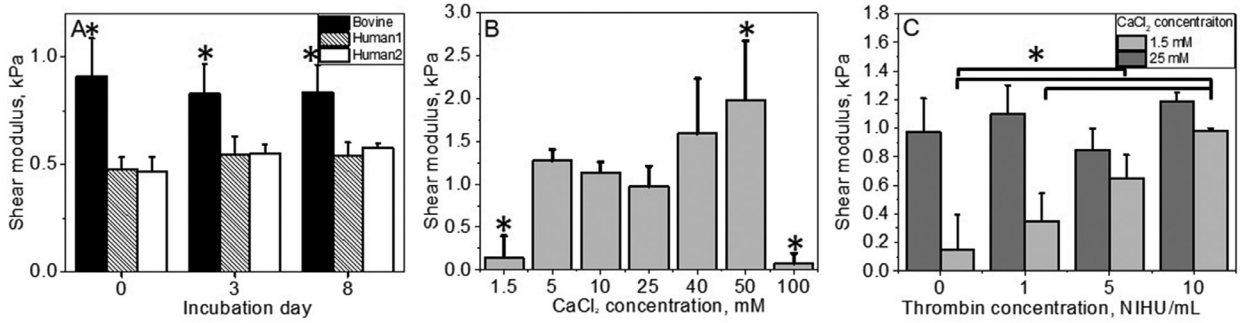

Fig. 3. Shear modulus measured with an indentometer in human and bovine hematoma phantoms. (a) Freshly clotted bovine (n = 4) and human (n = 4, human 1) blood and recalcified anticoagulated human blood (n = 6, human 2) incubated for 0−8 d. There were no statistically significant differences between shear moduli of any of the human blood groups or between any of the bovine blood groups. Shear moduli of all bovine blood groups were significantly higher than those of human blood groups, as per pairwise Student's *t*-test comparisons at the $p < 0.05$ level. (b, c) Anticoagulated bovine blood clotted by r adding calcium chloride (b) either alone or (c) in combination with varying concentrations of thrombin (n = 4−9). *Statistical significance at $p < 0.05$ in one-way analysis of variance; error bars represent standard deviations.

Although multiple types of plastics were used as molds for hematoma samples, and one might expect a range of retraction and stiffness because of the difference in surface charge, no differences were observed between samples prepared with an otherwise identical protocol, as measured with the indentometer. Further, in an additional set of measurements aimed at investigating the influence of container material and incubation temperature on hematoma stiffness and retraction over time, anticoagulated bovine blood was recalcified (at the final $CaCl_2$ concentration of 25 mmol/L) in either cylindrical borosilicate glass containers (group 1, n = 4) or cylindrical polypropylene containers (group 2, n = 4) of the same size (55 mL volume, 4 cm in diameter, 4 cm high) and incubated either at 36°C or at room temperature (group 3, polypropylene containers, n = 4) for 3 h. Measurements of stiffness with the indentometer and the degree of retraction were then performed. Thereafter, the samples were kept refrigerated for 3 d and re-tested. All samples in this set exhibited a consistent degree of retraction in the range 6%−12%, which did not change over the 3-d incubation period. There was no difference on either of the days in the stiffness of samples incubated in polypropylene containers and borosilicate glass containers (shear moduli of 0.95 ± 0.13 and 0.79 ± 0.05 kPa on day 0; 1.04 ± 0.03 and 0.98 ± 0.13 kPa on day 3, respectively), and the range of shear modulus values was consistent with that seen in Figure 3a and 3b. Further, shear moduli of samples prepared by incubation at room temperature did not differ from those incubated at 36°C for 3 h on neither of the time points.

Spatial distribution of shear modulus within a bovine clot sample of larger, clinically relevant size was also characterized by elasticity imaging (Fig. 4). The gray-scale B-mode image underlying the elasticity map clearly indicates the separation of organized and serous (liquid, hypo-echoic) fractions of the hematoma. The distribution of elastic modulus within the organized fraction, as seen in the elasticity map, was remarkably homogeneous, and the shear modulus was measured to be 1.04 ± 0.24 kPa. The values tended to be at the lower end of this range close to the boundary between organized and serous fractions, and at the higher end in the bulk of the sample. This is in agreement with SWE imaging reported previously for large-volume porcine blood clots (Bernal et al. 2012). Subsequent measurements of the shear modulus of the same sample with the indentometer yielded the value of 0.67 ± 0.08 kPa, which was similar to, but slightly lower than that measured by SWE imaging, which is likely owing to the elastic modulus being at the lower limit of the imaging machine's dynamic range.

Dependence of BH lesion dimensions on the clot shear modulus

In Figure 5a are representative images of BH lesions produced in bovine clots with shear moduli varying within the achievable range: 0.4−1.6 kPa. The softest samples, with shear moduli ≤0.4 kPa, were too mechanically weak to maintain shape and had to be placed directly into a thin plastic bag for treatment. Consequently, the BH lesions could not be accurately bisected for size measurement, and instead, their size was determined from the B-mode ultrasound image acquired after BH exposure. As seen, all lesions have a characteristic "tadpole" shape, with the HIFU focus located toward the proximal end of the narrow "tail," which is consistent with our prior observations (Khokhlova et al. 2016). The "tail" is clearly larger for softer clots, and so is the lateral size of the "head." However, the axial size of the "head" (*i.e.,* the distance from the transducer focus to the proximal side of the BH lesion) is remarkably similar for all samples and corresponds to the distance between the focus and the first axial null of the HIFU field, which, for this transducer, is equal to

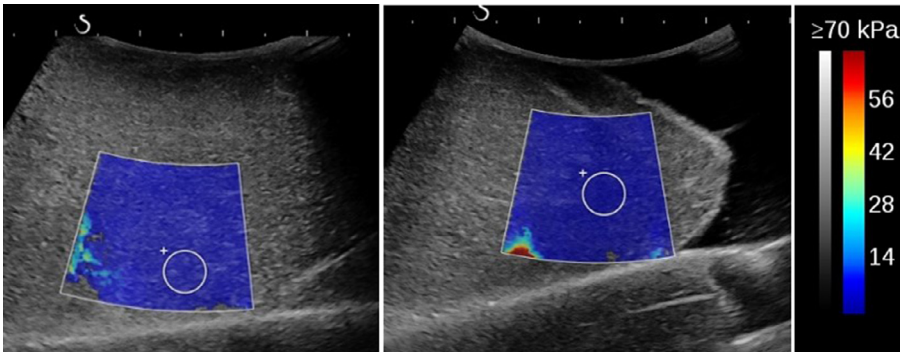

Fig. 4. Representative shear wave elastography (SWE) images of the large-volume bovine clot sample in the bulk (left) and close to the border (middle) of the organized and serous fractions of the clot. Color bar indicates elastic modulus, which, for soft tissues, is considered to be three times the shear modulus. The range of values for shear modulus, obtained from circular regions of interest, was similar to those obtained by direct indentometer measurements for this sample.

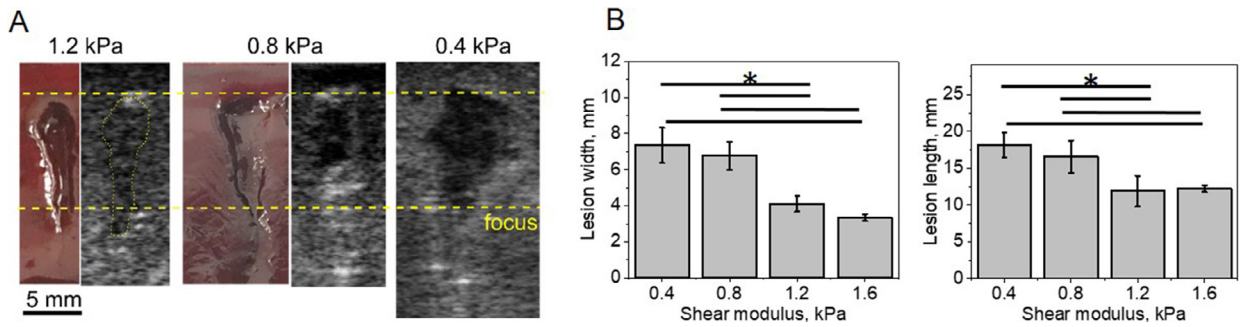

Fig. 5. (a) Representative photos and B-mode ultrasound images of BH cavities produced using thirty 10-ms pulses in clots with shear modulus varying within achievable limits. The high-intensity focused ultrasound (HIFU) was incident from the top of the images. The axial location of the HIFU focus is indicated by a *yellow dashed line*. (b) Maximum width (left) and length (right) of the cavities for various shear modulus ranges (n = 3−6). *Statistically significant difference between groups at $p < 0.05$. Error bars represent standard deviations.

10 mm (Khokhlova et al. 2018). The maximum lesion width (*i.e.,* the lateral size of the "head") significantly decreases with the increase in shear modulus 0.4−1.6 kPa by almost twofold (Fig. 5b); the overall length also significantly decreased within that range of shear modulus but not as substantially as the width (Fig. 5c). Interestingly, there appears to be a threshold-like behavior around the clot stiffness range of 0.8−1.2 kPa: lesion sizes are similar below and above that range. This intriguing behavior deserves further consideration.

DISCUSSION

The overarching goal of this work was to evaluate the feasibility of using BH to liquefy extravascular hematomas of different ages and to identify the *in vitro* phantom that would be representative of the stiffness (and, therefore, susceptibility to BH) of traumatic hematomas in humans. The process that was expected to contribute the most to changes in clot stiffness was the formation of fibrin matrix and its retraction over time (*i.e.,* separation of the clot into serous and organized fractions). This process should occur similarly *in vitro* and *in vivo* in the extravascular space, at least within the first week post-injury, as it is largely facilitated by signaling of the platelets and activity of the neutrophils already present in the clot volume, as opposed to remodeling by infiltrating leukocytes and fibroblasts (Rao et al. 2016b; Ryan et al. 1999). Further, in Rao et al. (2016b), the infiltration of fibroblasts and macrophages and formation of collagen were observed only within the narrow border at the surface of traumatic subdural hematomas, not in their bulk, up to 10 d post-injury. This further supports the relevance of the *in vitro* model to investigating the efficiency of BH in liquefaction of the bulk of acute and late subacute hematomas (≤10 d old). In this study, we used large volumes of clotted bovine and human blood as *in vitro* phantoms to evaluate the retraction by measuring the expunged serous volumes and stiffness changes *via* indentometer measurements within the time frame from 3 h to 8 d. The retraction was found to occur mostly within the first 3 h after clotting for all samples and did not significantly change over the subsequent week-long incubation period. The shear modulus of both human and bovine samples was remarkably independent of the degree of retraction and was noticeably lower than those of most human soft tissues with the exception of healthy liver parenchyma (Yeh et al. 2002). These results indicate that the organized fraction of a subacute hematoma should not be expected to become stiffer—and therefore harder to liquefy—than acute, non-retracted hematoma. Naturally clotted bovine blood samples were found to be almost twofold stiffer on average than human samples, which is in agreement with previously reported inter-species differences in clotting dynamics (Mizuno et al. 2018). Therefore, naturally clotted bovine blood used as an *in vitro* model in our previous BH studies was substantially stiffer than what could be anticipated clinically in traumatic hematomas and, therefore, represents a worst-case scenario in terms of the liquefaction rate.

Interestingly, the values of shear modulus for naturally clotted human samples measured here were lower than these measured by Mercado-Shekhar et al. (2018) for highly retracted intravascular *in vitro* clot models (0.55 ± 0.04 kPa vs. 1.07 ± 0.6 kPa), but higher than the values for mildly retracted clots reported in the same study (0.26 ± 0.06 kPa). This discrepancy indicates that the surface-to-volume ratio of the clot may play a role in the retraction process and in the resulting material stiffness. Further, the material of the container in which the clots were prepared—polypropylene (hydrophobic) and borosilicate glass (hydrophilic)—influenced neither the degree of retraction nor the shear modulus of the clot. Again, this contrasts with prior studies of intravascular clots with much higher surface-to-volume ratios, where clots were observed to retract only in containers made of

hydrophilic material—borosilicate glass (Sutton et al. 2013; Zhang et al. 2016). This indicates the reduced influence of container surface material in promoting the coagulation cascade in the present case of larger-volume clots with lower surface-to-volume ratio.

Not only is freshly clotted bovine blood stiffer than human clot, but its use as an *in vitro* phantom in BH experiments may also be logistically challenging and may not allow for molding hematomas into complex shapes, more representative of the clinical cases. It is therefore preferable to use anticoagulated bovine blood and to initiate clotting by adding concentrations of $CaCl_2$ and thrombin that replicate the shear modulus of fully retracted human hematoma. Indentometer measurements of shear moduli of the bovine blood clots obtained in this fashion indicated that the use of $CaCl_2$ alone, at concentrations of 10−40 mmol/L, leads to a shear modulus range similar to that of freshly clotted bovine blood. Interestingly, $CaCl_2$ concentrations both lower and higher than this range resulted in very soft, nearly liquid clots. At low $CaCl_2$ concentration (1.5 mmol/L), the addition of thrombin within the range 1−5 NIHU/mL had a slightly stiffening effect on the clot material, such that the shear modulus matched the range for retracted human hematoma. The softening effect of low and high $CaCl_2$ concentrations is consistent with electron microscopy observations of purified fibrin network (Ryan et al. 1999): higher concentrations of $CaCl_2$ lead to a fibrin network consisting of fewer, but thicker and longer fibrils, with lower branch-point density. Lower concentrations of $CaCl_2$ resulted in very high branch-point density, but thinner fibrils. Both greater branching and thicker fibrils were reported to have a stiffening effect on the clot. Therefore, in clots with intermediate fiber sizes and branch-point densities, these effects were expected to be balanced, and the clots would therefore have the highest stiffness. Although the present study did not include evaluation of the clots at the ultrastructural level, the presence of a fibrin network in the bulk of both human and bovine large-volume *in vitro* clots was revealed through scanning electron microscopy imaging by Ponomarchuk et al. (2019).

BH exposures of clots with varying shear moduli, prepared as described above, resulted in complete fractionation of the grossly homogenous clot structure at the focal area, forming liquid lesions 8−20 mm in length and 3−8 mm in width. The liquid contents could be easily aspirated or poured out of the otherwise homogeneously gelatinous sample, similarly to prior studies of BH liquefaction of hematomas and other soft tissues (Khokhlova et al. 2016, 2017). In the present study, the liquid content was not investigated histologically, but in our prior studies it was found to contain intact red blood cells, lysed red blood cells and fragments of fibrin network with or without embedded red blood cells $\leq$25 μm in size (Khokhlova et al. 2016). The lesion dimensions were larger for clots with lower shear modulus, as expected, regardless of the protocol used to achieve such shear modulus, for example, very high or very low concentration of $CaCl_2$, which hypothetically produced different clot structure at the microscopic level (Ryan et al. 1999). The lesion dimensions in stiffer clots (shear moduli of $\geq$1 kPa) were similar to those of BH lesions achieved with the same transducer in bovine liver, which is reported to have a similar shear modulus and to be similar to human liver as well (Yeh et al. 2002; Klatt et al. 2010). BH lesion dimensions, and therefore liquefied volume, are known to increase fairly monotonously with the number of pulses and then saturate at ~15−30 pulses for most soft tissues and hematoma material (Khokhlova et al. 2016). Therefore, the liquefaction rate, that is, the liquefied volume per unit time, will be larger for softer hematomas than for stiffer ones, regardless of the number of pulses used per focal spot.

The axial size of the lesion was less dependent on the shear modulus than the lateral size, which is also consistent with our previous observations of BH lesions in tissues of different stiffness—bovine liver and cardiac muscle tissues (Khokhlova et al. 2017). Remarkably, the distance between the HIFU focus and the proximal border of the lesion was the same for all lesions and corresponded to the distance from the focus to the first pre-focal null of the field; that is, only the length of the lesion "tail" decreased for stiffer clots. Whether this observation holds for HIFU transducers with different field structure remains to be seen and will be the subject of future studies.

SWE imaging of a large-volume *in vitro* clot prepared from recalcified anticoagulated bovine blood and incubated for 3 d revealed that the organized fraction of the retracted clot is very homogeneous in terms of elastic modulus distribution. Quantitatively, the average shear modulus measured with SWE was similar to that subsequently measured with the indentometer in the same sample and in agreement with that measured with SWE by Bernal et al. (2012) in large-volume porcine clot samples.

CONCLUSIONS

Elasticity of large-volume, naturally clotted bovine and human blood was found to be independent of incubation time (within 1 wk) or degree of retraction and was lower than that for most soft tissues, as measured with an indentometer and confirmed by shear wave elastography. The values of the shear moduli were quite consistent between different samples and over a sample volume, and were much higher for bovine blood than for human blood. The range of shear moduli for retracted human hematoma was best recapitulated by adding

1.5 mmol/L $CaCl_2$ and 1−5 NIHU/mL to anticoagulated whole bovine blood. The range of shear moduli for naturally clotted bovine blood could be best reproduced with anticoagulated bovine blood by adding $CaCl_2$ alone at 25 mmol/L concentration. BH liquefaction of the clot material was feasible in all samples, and the BH cavities were larger than those observed in soft tissues at the same *in situ* acoustic parameters, as expected because of the low shear modulus of the clots. These results support the expectation of BH liquefaction being clinically relevant for management of both acute and chronic hematomas. The dimensions of the BH cavities produced with the same exposure parameters were significantly dependent on the sample shear modulus within the range 0.4−1.6 kPa; the maximum width and overall volume of the cavity were more affected by the change in shear modulus than the maximum length, which is consistent with the hypothesized mechanisms of BH lesion formation—formation of vapor cavity, acoustic atomization into the cavity, pre-focal cavitation and streaming (Simon et al. 2012; Pahk et al. 2019).

Acknowledgments—We thank Pavel Trakhman and Nikolay Starostin from Dmitriy Rogachev Research Center for providing donor blood samples and Lomonosov Moscow State University students Ksenia Topchu and Anna Kunturova for help in measurements of human clot shear modulus. This work was supported in part by U.S. National Institute of General Medicine Grant R01 GM122859, U.S. National Institute of Biomedical Imaging and Bioengineering Grant R01 EB019365 and Russian Foundation for Basic Research Grant 20-02-00210.

Conflict of interest —The authors declare no conflicts of interest.

REFERENCES

Bernal M, Gennisson JL, Flaud P, Tanter M. Shear wave elastography quantification of blood elasticity during clotting. Ultrasound Med Biol 2012;38:2218–2228.

Bessonova O V, Khokhlova VA, Canney MS, Bailey MR, Crum LA. A derating method for therapeutic applications of high intensity focused ultrasound. Acoust Phys 2010;56:354–363.

Bollen V, Hendley SA, Paul JD, Maxwell AD, Haworth KJ, Holland CK, Bader KB. In vitro thrombolytic efficacy of single- and five-cycle histotripsy pulses and rt-PA. Ultrasound Med Biol 2019;46:336–349.

Choi I, Shield RT. Second-order effects in problems for a class of elastic materials. Z Angew Math Phys 1981;32:361–381.

Chueh JY, Wakhloo AK, Hendricks GH, Silva CF, Weaver JP, Gounis MJ. Mechanical characterization of thromboemboli in acute ischemic stroke and laboratory embolus analogs. Am J Neuroradiol 2011;32:1237–1244.

Dunmire B, Kucewicz JC, Mitchell SB, Crum LA, Sekins KM. Characterizing an agar/gelatin phantom for image guided dosing and feedback control of high-intensity focused ultrasound. Ultrasound Med Biol 2013;39:300–311.

Gerhardson T, Sukovich JR, Pandey AS, Hall TL, Cain CA, Xu Z. Effect of frequency and focal spacing on transcranial histotripsy clot liquefaction, using electronic focal steering. Ultrasound Med Biol 2017;43:2302–2317.

Gerhardson T, Sukovich JR, Chaudhary N, Chenevert TL, Ives K, Hall TL, Camelo-Piragua S, Xu Z, Pandey AS. Histotripsy clot liquefaction in a porcine intracerebral hemorrhage model. Neurosurgery 2020;86:429–436.

Khokhlova TD, Monsky WL, Haider YA, Maxwell AD, Wang YN, Matula TJ. Histotripsy liquefaction of large hematomas. Ultrasound Med Biol 2016;42:1491–1498.

Khokhlova TD, Haider YA, Maxwell AD, Kreider W, Bailey MR, Khokhlova VA. Dependence of boiling histotripsy treatment efficiency on HIFU frequency and focal pressure levels. Ultrasound Med Biol 2017;43:1975–1985.

Khokhlova T, Rosnitskiy P, Hunter C, Maxwell A, Kreider W, ter Haar G, Costa M, Sapozhnikov O, Khokhlova V. Dependence of inertial cavitation induced by high intensity focused ultrasound on transducer F-number and nonlinear waveform distortion. J Acoust Soc Am 2018;144:1160–1169.

Klatt D, Friedrich C, Korth Y, Vogt R, Braun J, Sack I. Viscoelastic properties of liver measured by oscillatory rheometry and multifrequency magnetic resonance elastography. Biorheology 2010;47:133–141.

Looi T, Khoklova V, Hynynen K, Drake J. A preliminary in-vivo porcine study of long pulse histotripsy for thrombolysis of intraventricular hemorrhagic clot. J Acoust Soc Am 2016;140:3031.

Maxwell AD, Yuldashev PV, Kreider W, Khokhlova TD, Schade GR, Hall TL, Sapozhnikov OA, Bailey MR, Khokhlova VA. A prototype therapy system for transcutaneous application of boiling histotripsy. IEEE Trans Ultrason Ferroelectr Freq Control 2017;64:1542–1557.

Mercado-Shekhar KP, Kleven RT, Aponte Rivera H, Lewis R, Karani KB, Vos HJ, Abruzzo TA, Haworth KJ, Holland CK. Effect of clot stiffness on recombinant tissue plasminogen activator lytic susceptibility in vitro. Ultrasound Med Biol 2018;44:2710–2727.

Mizuno T, Tsukiya T, Takewa Y, Tatsumi E. Differences in clotting parameters between species for preclinical large animal studies of cardiovascular devices. J Artif Organs 2018;21:138–141.

Nogueira RG, Levy EI, Gounis M, Siddiqui AH. The Trevo device: preclinical data of a novel stroke thrombectomy device in two different animal models of arterial thrombo-occlusive disease. J Neurointerv Surg 2012;4:295–300.

Pahk KJ, de Andrade MO, Gélat P, Kim H, Saffari N. Mechanical damage induced by the appearance of rectified bubble growth in a viscoelastic medium during boiling histotripsy exposure. Ultrason Sonochem 2019;53:164–177.

Pickering JW, Hewitt JA. The syneresis of blood clots. Q J Exp Physiol 1923;13:199–207.

Ponomarchuk EM, Buravkov SV, Rosnitskiy PB, Tsysar SA, Karzova MM, Kunturova AV, Topchu KD, Sapozhnikov OA, Khokhlova VA. Cytological and ultrastructural analysis of mechanically liquefied lesions generated using boiling histotripsy in a porcine model of hematoma ex vivo. Presented at the 19th International Symposium of ISTU/5th European Symposium of EUFUS. Barcelona, Spain51.. June 13−15Abstract Book.

Rao MG, Singh D, Vashista RK, Sharma SK. Dating of acute and subacute subdural haemorrhage: A histo-pathological study. J Clin Diagn Res 2016;10:HC01–HC07.

Ryan EA, Mockros LF, Weisel JW, Lorand L. Structural origins of fibrin clot rheology. Biophys J 1999;77:2813–2826.

Scherer GW. Mechanics of syneresis: I. Theory. J Non-Cryst Solids 1989;108:18–27.

Simon JC, Sapozhnikov OA, Khokhlova VA, Wang Y-N, Crum LA, Bailey MR. Ultrasonic atomization of tissue and its role in tissue fractionation by high intensity focused ultrasound. Phys Med Biol 2012;57:8061–8078.

Sutton JT, Ivancevich NM, Perrin SR, Vela DC, Holland CK. Clot retraction affects the extent of ultrasound-enhanced thrombolysis in an ex vivo porcine thrombosis model. Ultrasound Med Biol 2013;39:813–824.

Szabo TL. Diagnostic ultrasound imaging: Inside out. 2nd edition Waltham, MA: Academic Press; 2004.

Vlaisavljevich E, Kim Y, Owens G, Roberts W, Cain C, Xu Z. Effects of tissue mechanical properties on susceptibility to histotripsy-induced tissue damage. Phys Med Biol 2014;33:395–401.

Wang YN, Khokhlova TD, Buravkov S, Chernikov V, Kreider W, Partanen A, Farr N, Maxwell A, Schade GR, Khokhlova VA. Mechanical decellularization of tissue volumes using boiling histotripsy. Phys Med Biol 2018;63 235023.

Weiss S, Messner F, Huth M, Weissenbacher A, Denecke C, Aigner F, Brandl A, Dziodzio T, Sucher R, Boesmueller C, Oellinger R, Schneeberger S, Oefner D, Pratschke J, Biebl M. Impact of abdominal drainage systems on postoperative complication rates following liver transplantation. Eur J Med Res 2015;20:66.

Xie H, Kim K, Aglyamov SR, Emelianov SY, O'Donnell M, Weitzel WF, Wrobleski SK, Myers DD, Wakefield TW, Rubin JM. Correspondence of ultrasound elasticity imaging to direct mechanical measurement in aging DVT in rats. Ultrasound Med Biol 2005;31:1351–1359.

Yeh WC, Li PC, Jeng YM, Hsu HC, Kuo PL, Li ML, Yang PM, Lee PH. Elastic modulus measurements of human liver and correlation with pathology. Ultrasound Med Biol 2002;28:467–474.

Zhang X, Owens GE, Gurm HS, Ding Y, Cain CA, Xu Z. Noninvasive thrombolysis using histotripsy beyond the intrinsic threshold (microtripsy). IEEE Trans Ultrason Ferroelectr Freq Control 2015;62:1342–1355.

Zhang X, Owens GE, Cain CA, Gurm HS, Macoskey J, Xu Z. Histotripsy thrombolysis on retracted clots. Ultrasound Med Biol 2016;42:1903–1918.

Zhang X, Macoskey JJ, Ives K, Owens GE, Gurm HS, Shi J, Pizzuto M, Cain CA, Xu Z. Non-invasive thrombolysis using microtripsy in a porcine deep vein thrombosis model. Ultrasound Med Biol 2017;43:1378–1390.